JSLHR

Research Article

Influence of Left–Right Asymmetries on Voice Quality in Simulated Paramedian Vocal Fold Paralysis

Robin A. Samlan[a] and Brad H. Story[a]

Purpose: The purpose of this study was to determine the vocal fold structural and vibratory symmetries that are important to vocal function and voice quality in a simulated paramedian vocal fold paralysis.
Method: A computational kinematic speech production model was used to simulate an exemplar "voice" on the basis of asymmetric settings of parameters controlling glottal configuration. These parameters were then altered individually to determine their effect on maximum flow declination rate, spectral slope, cepstral peak prominence, harmonics-to-noise ratio, and perceived voice quality.
Results: Asymmetry of each of the 5 vocal fold parameters influenced vocal function and voice quality; measured change was greatest for adduction and bulging. Increasing the symmetry of all parameters improved voice, and the best voice occurred with overcorrection of adduction, followed by bulging, nodal point ratio, starting phase, and amplitude of vibration.
Conclusions: Although vocal process adduction and edge bulging asymmetries are most influential in voice quality for simulated vocal fold motion impairment, amplitude of vibration and starting phase asymmetries are also perceptually important. These findings are consistent with the current surgical approach to vocal fold motion impairment, where goals include medializing the vocal process and straightening concave edges. The results also explain many of the residual postoperative voice limitations.

People with unilateral vocal fold motion impairment (VFMI) secondary to vocal fold paresis or paralysis frequently seek evaluation and management of a weak, breathy voice. Surgical treatments improve voice quality by increasing closure of the glottal airspace during phonation, although some level of voice handicap or limitation often remains. A likely reason for continued dysphonia is residual asymmetries of vocal fold shape and muscle tone resulting in vibration asymmetries, a hypothesis examined in the current study.

Multiple structural and vibratory laryngeal asymmetries can occur with unilateral VFMI secondary to vocal fold paresis or paralysis. Reduced mobility of one arytenoid is the pathognomic feature of unilateral VFMI, with possible asymmetries of lateral–medial, superior–inferior, and anterior–posterior arytenoid position. Other asymmetries of structure and gross function include an ipsilaterally enlarged ventricle, bowed (i.e., concave) edge, thinned immobile fold, vertical plane difference at rest or during phonation, and tilting toward the intact side (Isshiki & Ishikawa, 1976; Yamada, Hirano, & Ohkubo, 1983; Yumoto, Nakano, & Oyamada, 2003). People with VFMI often present with constriction of the supraglottis in the form of anterior–posterior constriction and/or medial movement of the ventricular folds, particularly the contralateral ventricular fold (Bielamowicz, Kapoor, Schwartz, & Stager, 2004; Pinho, Pontes, Gadelha, & Biasi, 1999).

The left–right differences in structure, gross function, and muscle tone can lead to incomplete glottal closure, left–right and anterior–posterior vibratory asymmetry, aperiodic vibration, and altered amplitude of vibration and mucosal wave (Eysholdt, Rosanowski, & Hoppe, 2003; Hirano & Mori, 2000; Kokesh, Flint, Robinson, & Cummings, 1993; Omori, Slavit, Kacker, Blaugrund, & Kojima, 2000; Schwarz et al., 2006). Left–right vibratory asymmetries (i.e., phase differences) and frequency differences between the vocal folds have been documented, sometimes shifting over time or increasing in magnitude and then resetting (von Leden & Moore, 1961; Wittenberg, Tigges, Mergell, & Eysholdt, 2000). Smaller vocal fold velocity and acceleration have

[a]Department of Speech, Language, and Hearing Sciences, University of Arizona, Tucson
Correspondence to Robin A. Samlan: rsamlan@email.arizona.edu
Editor: Julie Liss
Associate Editor: Jack Jiang
Received February 24, 2016
Revision received May 3, 2016
Accepted May 31, 2016
DOI: 10.1044/2016_JSLHR-S-16-0076

Disclosure: *The authors have declared that no competing interests existed at the time of publication.*

also been reported for paralyzed folds compared with healthy folds (Lohscheller & Eysholdt, 2008).

The asymmetries might lead to slower opening and closing of the glottal airspace and a shorter time period during which the airspace is maximally closed, observed as a more rounded glottal area (A_g) waveform with a longer open quotient. A more rounded A_g will likely cause the glottal flow (U_g) to be closer to a sinusoid, although the anatomic and functional differences in supraglottal shape and vocal tract inertance also influence U_g. A nearly sinusoidal U_g, with its associated gradual U_g shut-off, has been hypothesized to lead to higher amplitude of the fundamental frequency (H1) relative to other harmonics, energy loss causing increased first formant bandwidth, and rapid drop-off of harmonic amplitude across the source and acoustic spectra (Fischer-Jørgensen, 1967; Hillenbrand, Cleveland, & Erickson, 1994; Huffman, 1987). Complicating these expected spectral changes, turbulent flow will likely lead to noise in the region of the third formant (F3; Hillenbrand et al., 1994; Klatt & Klatt, 1990). As a group, these changes are consistent with breathy voice quality (Fischer-Jørgensen, 1967; Hillenbrand et al., 1994; Huffman, 1987; Klatt & Klatt, 1990) along with decreased loudness, roughness, diplophonia, asthenia, high pitch, and strain (Billante, Clary, Childs, & Netterville, 2002; Hartl, Hans, Vaissière, & Brasnu, 2003; Kiritani, Hirose, & Imagawa, 1993).

Injection laryngoplasty, medialization thyroplasty, and arytenoid adduction—three mainstays of treatment for unilateral VFMI—improve voice quality by altering the position and contour of the edge of the immobile vocal fold, thus increasing closure of the glottal airspace during phonation. These procedures are generally effective in improving voice quality, but they do not always facilitate return to normal function. In one study, for example, 92% of 15 patients reported more than 1 year after thyroplasty that the surgery improved their voice, yet only 13% were extremely happy with their postoperative voice (Gray, Barkmeier, Jones, Titze, & Druker, 1992), citing continued challenges in achieving adequate loudness, quality differences (e.g., breathiness and hoarseness), altered sensations (e.g., a need to clear the throat or throat tension), and functional limitations (e.g., fatigue or needing to modify job responsibilities; Gray et al., 1992). Hogikyan, Wodchis, Terrell, Bradford, and Esclamado (2000) reported that the voice-related quality of life scores were higher (better) for patients with vocal fold paralysis treated with type I thyroplasty than for patients with untreated paralysis yet not as high as for controls with a typical voice. Leder and Sasaki (1994) reported that the number of breath groups during a standard reading passage was higher for patients after thyroplasty than for normophonic controls.

Comparing patients with unilateral VFMI to a normative data set, Billante et al. (2002) found that voices were commonly rated as mildly breathy 12 months after medialization thyroplasty with or without arytenoid adduction. Maximum phonation time, frequency range, jitter, and shimmer remained abnormal, although intensity and mean airflow rate returned to the normal range (Billante et al., 2002). In another study, pretreatment to posttreatment improvement in postoperative voice quality, stroboscopic ratings, and voice handicap were reported for injection laryngoplasty using calcium hydroxylapatite or micronized acellular dermis and for medialization thyroplasty with or without arytenoid adduction. Posttreatment values generally remained outside normal ranges (Lundy, Casiano, McClinton, & Xue, 2003). Thompson, Maragos, and Edwards (1995) reported improvements in glottal closure, amplitude of vibration, and mucosal wave after thyroplasty with or without arytenoid adduction, and six of the nine patients demonstrating preoperative asymmetric vibration continued to have asymmetric vibration postoperatively.

It is proposed that continued dysphonia is due to residual asymmetries of vocal fold shape and muscle tone with subsequent asymmetric vocal fold vibration. The effects of individual structural and vibratory vocal fold asymmetries when all other parameters were fully symmetric were described in Samlan, Story, Lotto, and Bunton (2014). When vocal process adduction, edge bulging, or nodal point ratio (R_{zn}; an estimate of the pivot point of the rotational vibratory mode) was the only asymmetry present, the asymmetric parameter led to perceived changes in voice quality. Isolated vibratory phase or amplitude asymmetries did not cause perceivable changes in voice quality (Samlan et al., 2014). Although it is important to understand the functional outcomes of individual parameter deviations from symmetry, it became clear during early work that the functional effects of any particular parameter manipulation were dependent on the settings of the other parameters.

Continued subtle asymmetries of a group of vocal fold structural and vibratory parameters are hypothesized to explain some of the postoperative variability in vocal fold vibration and voice quality situations in which glottal closure appears adequate yet patients continue to experience functional limitations of VFMI. The first aim of this study was to assess the vocal function effects of a constellation of slight asymmetries, none of which alone produced dramatic changes in vocal function or voice quality. Three asymmetries were programmed into a kinematic vocal fold model, creating an asymmetric exemplar. Model output was compared to the results generated using fully symmetric settings. It was expected that these minimal asymmetries would cause measurable differences in vocal function compared with the fully symmetric case.

The second aim was to determine how systematically modifying the symmetry of each of the five model parameters would alter the vocal function and voice quality of the asymmetric exemplar. It was hypothesized, contrary to findings when the exemplar was fully symmetric (Samlan et al., 2014), that all five parameters would affect vocal function and voice quality.

The speech production model consisted of a kinematic vocal fold model (Titze, 1984, 1989, 2006) aerodynamically and acoustically coupled to a wave reflection model of the trachea and vocal tract (Liljencrants, 1985; Story, 1995, 2005; Titze, 2002) configured in the /a/ vowel shape described in Story (2008). The model is depicted in Figure 1. In this

Figure 1. Vocal fold model.

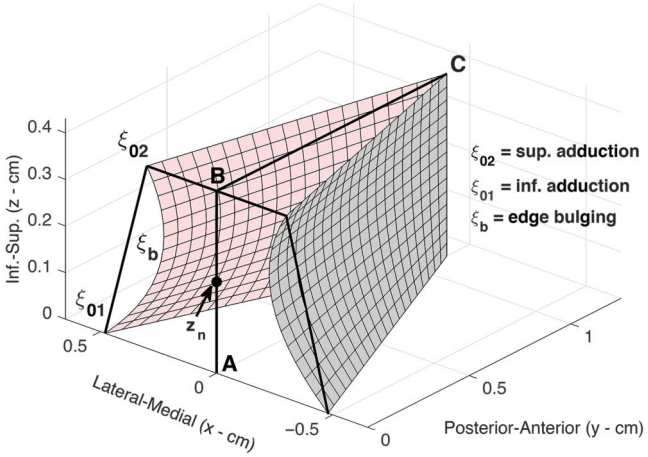

model, U_g is produced by the interaction of the A_g with the acoustic pressures in the trachea and vocal tract. As detailed in previous publications, a noise component was added to the U_g when the Reynolds number within the glottis exceeded 1,200 (Samlan & Story, 2011; Samlan, Story, & Bunton, 2013). All simulations were completed using a vocal tract consistent with a male adult and a fundamental frequency of 100 Hz.

Five parameters specifying the left and right vocal fold surfaces were set independently. Brief descriptions of the parameters are provided in Table 1, and additional detail about each parameter can be found in Samlan et al. (2014). The parameters modified included (a) adduction (ξ_{02}); (b) edge bulging (ξ_b); (c) nodal point (z_n), represented as the ratio of the z_n to the thickness of the folds (z_n/T, or R_{zn}); (d) amplitude of vibration (Asym); and (e) starting phase (φ).

Method

The purpose of Experiment 1 was to determine the effects of a combination of minimal asymmetries on voice production and vocal function. An asymmetric exemplar "speaker" was created using the kinematic speech production model described in the introduction. Parameter settings for the exemplar, or base, voice are listed in Table 2, and animations of their simulated vibration can be viewed in online Supplemental Video S2 and compared to the fully symmetric vibration shown in Supplemental Video S1. Three asymmetries were imposed to be consistent with a slight difference in left and right laryngeal muscle innervation (i.e., vocal fold paralysis): (a) The left ξ_b value was 0 cm so that the left edge was flat and the right edge was slightly convex at ξ_b = 0.1 cm, (b) the R_{zn} was slightly lower for the left (R_{zn} = .6) than the right (R_{zn} = .8), and (c) an 80° φ difference was introduced (left φ = 1.4 radians, right φ = 0 radians). Vocal process position and Asym were symmetric (left and right ξ_{02} = 0.1 cm, Asym = 1.0). The asymmetric base voice was compared to a fully symmetric base voice in which the settings for the left vocal fold surface were identical to those shown in Table 2 for the right fold. Comparison of the asymmetric and symmetric voices was completed through examination of A_g, U_g, and output pressure (P_{out}; analogous to the microphone signal) waveforms and spectra.

Five acoustic measures were computed from P_{out}. Maximum flow declination rate (MFDR) was measured from the derivative of U_g. The first and second harmonic amplitudes were measured using a peak-picking algorithm (Titze, Horii, & Scherer, 1987) and corrected for the amplitude of the first formant as described by Hanson (1997),

Table 1. Speech production model parameters.

Symbol	Parameter name and description	Definition
ξ_{02}	Adduction, vocal process separation	Distance (in millimeters) of the superior aspect of the vocal process from midline during vibration. Larger values reflect vocal process positioning farther from midline.
ξ_b	Bulging, edge contour	Curvature of the medial surface of the vocal fold in the vertical dimension. Likely reflects thyroarytenoid muscle contraction (Alipour & Scherer, 2000). Expected value in a healthy vocal fold is approximately 0.1 to 0.2 mm (Titze, 2006). Decreased ξ_b means a less-curved edge; negative ξ_b indicates a concave (i.e., bowed) edge.
R_{zn}, z_n/T	Nodal point ratio, pivot point ratio	Nodal point is the pivot point around which the rotational mode changes phase. Represented as the ratio of the nodal point to the thickness of the folds (z_n/T). The normal value is not known. A high nodal point indicates greater vibratory mass and larger amplitude of the lower portion of the folds (Titze & Story, 2002).
Asym	Asymmetry, left amplitude of vibration, amplitude asymmetry	The amplitude of vibration of the right vocal fold surface was determined by rule on the basis of vocal fold length, lung pressure, and threshold pressure (Titze, 2006). Amplitude of left vocal fold surface was scaled as a percentage of the right. A value of 1 indicates equal amplitude.
φ	Starting phase	Difference (in radians) in timing between lateral–medial movements of the two folds. Both surfaces set at φ = 0 radians indicates that the vocal fold surfaces move as mirror images so that they are at midline and maximum amplitude at the same time instants as one another.

Table 2. Parameter values for the baseline voice.

Parameter	Right vocal fold surface	Left vocal fold surface	Range (left vocal fold surface)
ξ_{02} (cm)	0.10	0.10	0.40 to –0.01
ξ_b (cm)	***0.10***	***0.00***	***–0.05 to 0.15***
R_{zn}	***.8***	***.6***	***.1 to .9***
Asym	n/a	1.0	0 to 1.0
φ (radians)	***0***	***1.4***	***2.4 to 0.0***

Note. The italicized values were asymmetric. ξ_{02} = adduction; ξ_b = bulging; R_{zn} = nodal point ratio; Asym = asymmetry; φ = starting phase; n/a = not applicable.

and their difference was computed (H1*-H2*). Mean root-mean-square energy was calculated for three frequency bands of the P_{out} spectra: 59 to 398 Hz (B0), 395 to 2003 Hz (B1), and 2003 to 5001 Hz (B2). Two measures of spectral tilt were computed from these bands: B0-B1 and B0-B2 (de Krom, 1995; Hartl et al., 2003). The cepstral peak prominence (CPP) was measured from the cepstrum of P_{out} using VoiceSauce, implemented in MATLAB (Shue, Keating, Vicenik, & Yu, 2011; downloaded from http://www.phonetics.ucla.edu/voicesauce/). VoiceSauce calculates CPP on the basis of the method described by Hillenbrand et al. (1994). The harmonics-to-noise ratio (HNR) was calculated for a 250-ms steady-state segment of P_{out} using a Praat script (Boersma, 1993; Boersma & Weenink, 2011).

The purpose of Experiment 2 was to determine the acoustic and perceptual effects of systematically modifying the asymmetry of one parameter while others remained slightly asymmetric. The speech production model was programmed to produce 30 different steps of each of the five previously described parameters (ξ_{02}, ξ_b, R_{zn}, Asym, and φ) while the remaining variables were maintained at their base settings (see the middle two columns of Table 2). The ranges through which the left surface was manipulated are found in the final column of Table 2. The 30 productions of each variable led to 150 unique /a/ vowels. The A_g, U_g, and P_{out} for each simulation were simultaneously collected. The effects of the five kinematic model parameters on the six measures of vocal function were assessed qualitatively.

Twenty naïve listeners were recruited from the general population at the University of Arizona. All study procedures were approved by the University of Arizona Institutional Review Board. Every listener was at least 18 years of age and passed a 25 dB HL hearing screening at 0.5, 1.0, 2.0, and 4.0 KHz (American Speech-Language-Hearing Association, 1997).

The perceptual consequences of worsening or improving each model parameter individually were assessed using a visual sort-and-rate task (Esposito, 2010; Granqvist, 2003; Samlan & Kreiman, 2014). Each of the 20 listeners rated every sample. The listeners rated the samples through a series of six separate rating tasks presented in a randomized order. The stimuli for five of the rating tasks were 15 audio signals for a specific parameter, equally spaced across the range listed in Table 2. Icons representing and linked to each of the 15 audio files were displayed on a monitor. Participants were instructed to arrange icons from worst voice to best voice, with the physical distance between the shapes representing the degree of difference. The parameter group and stimuli order were randomized for each listener, and stimuli were represented by randomly selected icons (see Figure 2). Responses were coded by distance from the left end point; stacked stimuli were assigned the same value.

In a sort-and-rate task, the distances among the stimuli relate only to those judged within the same task. Because it is not possible to compare stimuli across tasks (e.g., how the best voice achieved through improving symmetry of vibratory amplitude compares with the best voice simulated using increased ξ_b), a sixth sort-and-rate task using three settings of each of the five parameters was created. The settings represent the most asymmetric, middle, and most "corrected" values.

Ratings were analyzed using PROXSCAL multidimensional scaling (MDS). Stepwise linear regressions were completed for each of the rating tasks to determine which of the acoustic measures explained the most variance in the MDS coordinates. Statistical analysis was completed using SPSS Statistics Version 20 (IBM, Armonk, NY).

Results

Experiment 1: Comparison of Asymmetric to Fully Symmetric Exemplar

The mildly impaired exemplar used in the current study ("asymmetric") was compared to the fully symmetric exemplar to determine the combined effects of the three small asymmetries. Figure 3a shows the schematic of the model at maximum contact for the symmetric (left column) and asymmetric (right column) cases. Left and right vocal processes are positioned 0.1 cm from midline for both cases. Observe that the edge contour (ξ_b) is symmetric in the image on the left, and the left surface is flat (ξ_b = 0 cm) in the image on the right. In the section above the surfaces, contact area is shown in red and A_g is shown in blue, and the particular location in the vibratory series is given by the end point in each trace (i.e., maximum contact and minimum area).

Figure 3b shows four cycles of the A_g (symmetric on the left and asymmetric on the right), and Figure 3c shows the time derivative of the glottal area (dA_g/dt, which hereafter is referred to as dA_g for simplicity). Measures of these waveforms are compared in Table 3. Quotients were calculated using a baseline of 10% peak-to-peak amplitude. The maximum negative peak of dA_g is the maximum area declination rate. Note that the mild ξ_b, R_{zn}, and φ asymmetries of the asymmetric exemplar increased maximum and minimum area, led to a longer open phase, and decreased the closing velocity relative to the symmetric case.

The interaction of A_g with the vocal tract led to skewed U_g relative to A_g (see Figure 3d). Compared with the symmetric signal, increased minimum and maximum

Figure 2. Sort and rate task. Each shape was linked to an audio file. The shapes were dragged from the top half of the screen (where the blue rectangle and oval shapes are sitting) down to the horizontal line and arranged in order from the worst voice (left) to the best voice (right). The physical distance between the shapes represents the degree of difference.

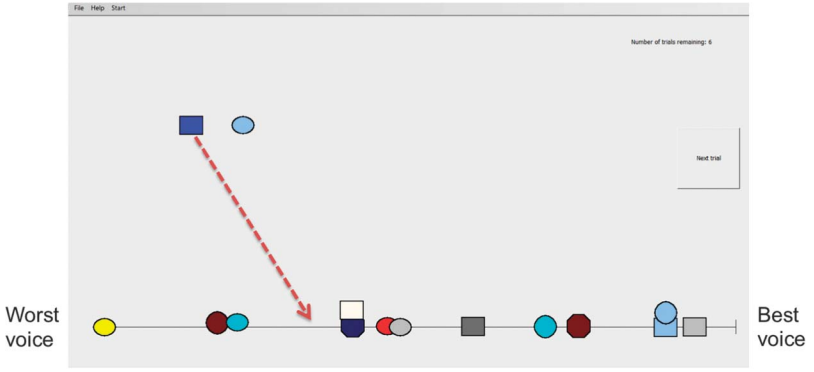

flow, more sinusoidal flow, and decreased MFDR were measured for the asymmetric exemplar (see Table 3). Glottal flow spectral slope was steeper for the asymmetric exemplar, with noise replacing harmonic energy after approximately 500 Hz (see Figure 3f).

The pressure signal radiated from the lips (P_{out}; see Figure 3g) results from interaction of the U_g with the pressures and shape of the vocal tract. Audio files of these signals can be found in the online supplemental materials. Compared with the P_{out} of the symmetric voice, the P_{out} for the asymmetric voice demonstrated reduced amplitude of the periodic component and smaller magnitude of the primary negative pressure pulse. The P_{out} spectrum (see Figure 3h) of the asymmetric voice revealed a steeper spectral slope and less prominent formants than that of the symmetric exemplar. Acoustic measures reflected these changes: H1*-H2* and B0-B1 increased, and B0-B2, CPP, and HNR decreased (see Table 3). Note that the B0-B2 was grouped with CPP and HNR because it likely represents increased noise energy in the B2 region.

In summary, these minimal asymmetries of ξ_b, R_{zn}, and phase led to changes in all signals compared with a fully symmetric exemplar. A_g became more rounded, U_g became more sinusoidal with an offset flow, and MFDR decreased. The spectral slope became steeper in the low frequencies, and inharmonic energy replaced harmonic energy in the higher frequencies.

Experiment 2: Symmetry Modifications

In this experiment, the effects of increasing and eliminating individual asymmetries were determined by sweeping each of the five left-sided parameters through the range of values listed in the rightmost column of Table 2 one at a time while all other parameters remained set as specified for the asymmetric exemplar (see the two middle columns of Table 2). The changes to vocal function measures are described below, followed by changes to perceived voice quality.

Relation of Asymmetries to Vocal Function Measures

The changes that occurred in each of the six vocal function measures as a particular model parameter was modified are shown in Figures 4 through 8. In each figure, the model parameter is on the *x*-axis; the most asymmetric value is at the left side of the graph and the most "corrected" value is at the right. Changing the parameter values from those at the left to those at the right, therefore, was always expected to improve vocal function. One vocal function measure is on the *y*-axis for each panel. Table 4 lists the best (maximum or minimum, as appropriate) value of every vocal function measure for the five parameters so that the changes occurring as the result of the individual parameter corrections can more easily be compared to the remaining parameters.

Adduction ξ_{02} asymmetries. The influence of ξ_{02} on measures of vocal function was evident when left ξ_{02} was set to 0.4 cm, then decreased to symmetry (ξ_{02} = 0.1 cm) and continued past midline to ξ_{02} = −0.1 cm (see Figure 4). MFDR increased 128,626 cm^3/s^2 to a maximum value of 156,180 cm^3/s^2 as ξ_{02} decreased from 0.40 cm (left border of the figure) to −0.07 cm. H1*-H2* decreased by 22.2 dB to a minimum of −2.9 dB as ξ_{02} decreased from 0.4 cm to −0.1 cm. The ratio B0-B1 increased 20.5 dB as ξ_{02} decreased from 0.40 cm to 0.09 cm (near the symmetric ξ_{02} value), reaching a maximum of 11.3 dB before decreasing 16.5 dB to a minimum of −4.8 dB at ξ_{02} = −0.1. Spectral slope measure B0-B2 increased by 33.1 dB to a maximum of 22.6 dB as ξ_{02} decreased from 0.40 cm to −0.07 cm, then decreased by 12.5 dB as left ξ_{02} continued to decrease. CPP increased by 20.3 dB to a maximum of 35.9 dB as ξ_{02} decreased from 0.4 cm to −0.1 cm. The sharpest increase in CPP occurred from approximately ξ_{02} = 0.05 cm to ξ_{02} = −0.10 cm. HNR increased by 42.8 dB to a maximum of 42.8 dB as ξ_{02} decreased from 0.4 cm to −0.1 cm. Most of that increase (37.5 dB) occurred between the ξ_{02} settings of 0.05 and −0.10 cm.

In summary, as ξ_{02} for the asymmetric exemplar decreased from 0.4 cm to −0.1 cm, MFDR, CPP, HNR, and B0-B2 increased and H1*-H2* decreased. These findings

Figure 3. Figures in the left column are results of the symmetric exemplar, and figures in the right column are results of the asymmetric exemplar. (a) Model schematic at maximum glottal closure. (b) Glottal area (A_g). (c) Derivative of the glottal area (dA_g). (d) Glottal flow (U_g). (e) Derivative of the glottal flow (dU_g). (f) Spectrum of the glottal flow. (g) Output pressure (P_{out}). (h) Spectrum of the output pressure.

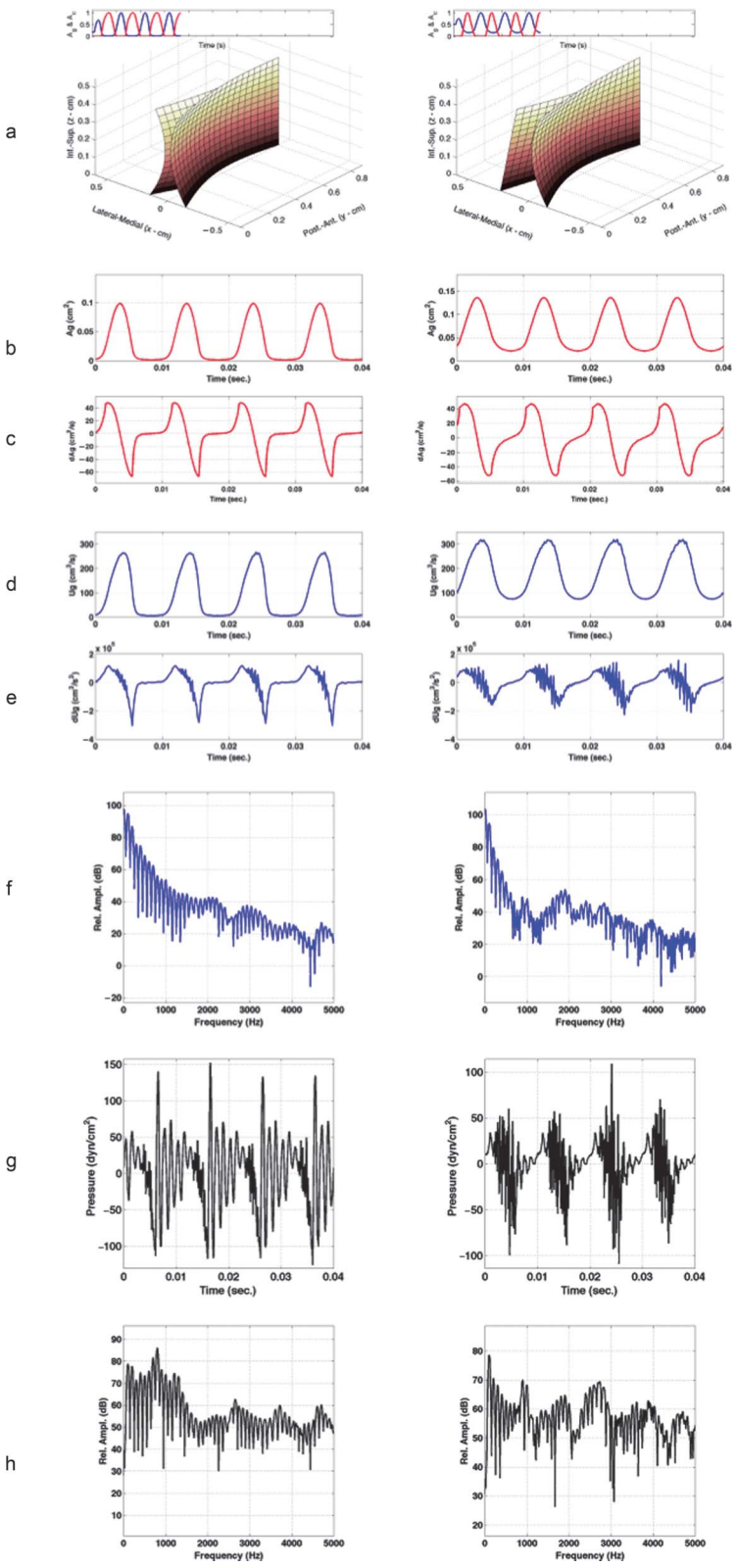

Table 3. Vocal function measures for exemplar voices.

Measure	Symmetric	Asymmetric
Maximum A_g (cm^2)	0.10	0.14
Minimum A_g (cm^2)	~0.00	0.02
A_g Q_o	0.46	0.60
A_g Q_s	1.20	0.99
MADR (cm^2/s)	67.0	52.5
Maximum U_g (cm^3/s)	265.4	317.0
Minimum U_g (cm^3/s)	9.2	74.0
U_g Q_o	0.49	0.66
U_g Q_s	1.6	1.3
MFDR (cm^3/s^2)	194,279	124,777
H1*-H2* (dB)	1.5	8.5
CPP (dB)	25.2	18.7
B0-B1 (dB)	0.1	11.4
B0-B2 (dB)	19.3	10.9
HNR (dB)	15.0	2.4

Note. A_g = glottal area; Q_o = open quotient; Q_s = speed quotient; MADR = maximum area declination rate; U_g = glottal flow; MFDR = maximum flow declination rate; H1*-H2* = the amplitude difference of the first and second harmonics, corrected for the amplitude of the first formant; CPP = cepstral peak prominence; B0-B1 = the amplitude difference of two frequency bands, B0 and B1; B0-B2 = the amplitude difference of two frequency bands, B0 and B2; HNR = harmonics-to-noise ratio.

are consistent with decreasing severity of dysphonia with decreasing vocal process separation. Most of the increase in CPP and HNR occurred when the left ξ_{02} was set at or medial to the symmetric value.

Bulging (ξ_b) asymmetries. In the asymmetric exemplar, the baseline setting for ξ_b was 0 cm. The effects of decreasing left ξ_b to −0.05 cm and increasing it to 0.15 cm are found in Figure 5. Decreasing left ξ_b to −0.05 cm decreased MFDR by 21,372 cm^3/s^2, and increasing left ξ_b from −0.05 cm to 0.15 cm increased MFDR by 45,768 cm^3/s^2 to a maximum MFDR of 154,606 cm^3/s^2. Decreasing ξ_b from 0 cm to −0.05 cm increased H1*-H2* by 2.7 dB. H1*-H2* decreased by 8.5 dB to a minimum of 2.4 dB as ξ_b increased from −0.05 cm to 0.15 cm. B0-B1 decreased by 0.3 dB when ξ_b decreased from 0 cm to −0.05 cm and decreased by 8.6 dB to a minimum of 2.1 dB as ξ_b increased from −0.05 cm to 0.15 cm. B0-B2 decreased by 2.8 dB as ξ_b decreased from 0 cm to −0.05 cm and increased by 11.5 dB to a maximum of 20.5 as ξ_b increased from −0.05 cm to 0.05 cm. CPP decreased by 1.1 dB as left ξ_b decreased to −0.05 cm and increased by 7.5 dB as ξ_b increased from −0.05 cm to 0.15 cm. HNR decreased by 2.4 dB as left ξ_b decreased to −0.05 cm and increased by 16.4 dB as ξ_b increased from −0.05 cm to 0.15 cm.

In summary, increasing the convexity of the vocal fold edge from ξ_b = −0.05 cm to 0.15 cm caused changes in MFDR and the spectrum consistent with decreasing severity of dysphonia. MFDR, B0-B2, CPP, and HNR increased, whereas H1*-H2* and B0-B1 decreased. Values did not reach those attained through decreasing ξ_{02}.

Nodal point ratio (R_{zn}) asymmetries. The left R_{zn} was both decreased and increased from the base value of .6, whereas the right R_{zn} was maintained at .8. Results are shown in Figure 6. MFDR was lowest (118,001 cm^3/s^2) at R_{zn} = .43, and it increased from that midthickness location by 24,622 cm^3/s^2 as R_{zn} decreased to .1 and by 32,315 cm^3/s^2 to a maximum of 150,316 cm^3/s^2 as R_{zn} increased to .9. The highest H1*-H2* (17.3 dB) occurred at R_{zn} = .21. H1*-H2* decreased by 0.8 dB as R_{zn} decreased to .1 and by 11.6 dB as R_{zn} increased to .9, where it reached its lowest value of 5.7 dB. The highest B0-B1 (11.6 dB) occurred at R_{zn} = .51. A 1.7-dB decrease occurred as R_{zn} decreased to .1, and a 5.2-dB decrease occurred as R_{zn} increased to .9. The lowest B0-B2 was 8.8 dB at R_{zn} = .16, with B0-B2 increasing 0.4 dB as R_{zn} decreased to .9 and B0-B2 increasing 5.6 dB as R_{zn} increased to .9. The minimum CPP of 16.9 dB occurred at R_{zn} = .38. CPP increased by 1.4 dB as R_{zn} decreased to .1 and increased 5.2 dB to a maximum CPP of 22.4 dB as R_{zn} increased to .9. HNR increased by 6.9 dB to a maximum of 6.8 dB as R_{zn} increased from .1 to .9. Most of this increase occurred between R_{zn} settings of .6 and .9.

In summary, increasing left R_{zn} from the lowered setting of the asymmetric exemplar caused MFDR, CPP, B0-B2, and HNR to increase and H1*-H2* and B0-B1 to decrease. Returning the left vocal fold to a higher R_{zn} improved vocal function even in the setting of persistent ξ_b and phase asymmetries.

Amplitude of vibration (Asym) asymmetries. The Asym value for the asymmetric exemplar was 1.0, indicating no baseline amplitude asymmetry. For this group of simulations, the vibratory amplitude of the left surface was set to 0% of that of the right surface (Asym = 0) and then gradually increased until it was equal to the amplitude of the right surface (Asym = 1). With the return to symmetry, changes in acoustic measures were small (see Figure 7). MFDR increased 50,348 cm^3/s^2 to a maximum of 124,777 cm^3/s^2. H1*-H2* decreased 3.1 dB to a minimum of 8.5. B0-B1 varied by 1.0 dB over the Asym range. B0-B2 increased by 2.2 dB, CPP increased by 3.7 dB, and HNR increased by 1.4 dB.

In summary, decreasing left Asym to 0 in the context of the asymmetric base voice produced very small changes in vocal function that improved as vibratory amplitude was gradually increased. As left amplitude increased from 0% to 100% of that of the right, H1*-H2* decreased and MFDR, B0-B2, CPP, and HNR increased.

Starting phase (φ) asymmetries. The left and right folds were out of phase by 1.4 radians for the asymmetric base voice. As observed in Figure 8, the lowest MFDR occurred when the left φ was 2.40 radians and MFDR increased 63,310 cm^3/s^2 to a maximum of 140,353 cm^3/s^2 as left φ decreased to 0 (i.e., symmetric). Over the same range of φ values, H1*-H2* decreased 11.1 dB to a minimum of 5.4 dB, B0-B1 decreased by less than 1.0 dB, and B0-B2 increased by 3.5 dB to a maximum of 12.5 dB. CPP increased 4.0 dB to 20.1 dB as φ returned to symmetry, and HNR increased 2.4 dB to its maximum value of 3.1 dB at 0.76 radians.

As with symmetry of vibratory amplitude, increasing the vibratory phase difference between the folds worsened vocal function. Even the 1.40-radian phase shift present in the asymmetric base voice influenced vocal function, as

Figure 4. Changes in vocal function measures with decreasing left adduction (ξ_{02}): (a) maximum flow declination rate (MFDR); (b) the amplitude difference of the first and second harmonics, corrected for the amplitude of the first formant (H1*-H2*); (c) the amplitude difference of two frequency bands, B0 and B1 (B0-B1); (d) the amplitude difference of two frequency bands, B0 and B2 (B0-B2); (e) cepstral peak prominence (CPP); and (f) harmonics-to-noise ratio (HNR).

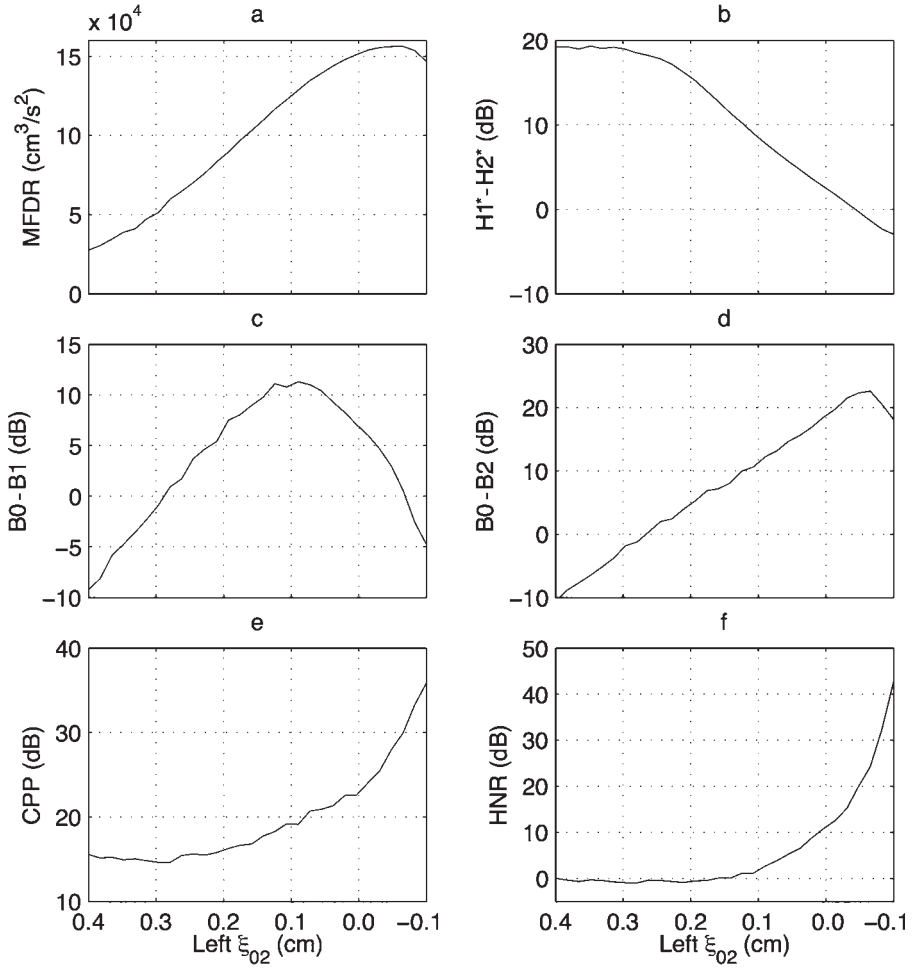

seen through improved measures with increased symmetry. As with amplitude asymmetry, the effect was much smaller than for the other three parameters.

Relation of Individual Asymmetries to Perception

Comparative influence of individual parameters on perceived quality. The relative influence of each of the parameters on perceived overall voice quality was determined using MDS. A one-dimensional solution fit the data well for each model parameter. Dispersion accounted for was greater than or equal to 0.97, indicating that the distances in the solution described at least 97% of the variance in the ratings. Although the direction of ratings is not maintained in the MDS solutions, mean ratings were higher for the most corrected sample (sample 15) than for the most asymmetric sample (sample 1) for all five parameters rated. For ease of interpretation, MDS solutions therefore are displayed so that the samples rated lowest are on the left side of the figure and those rated highest are on the right side.

Adduction (ξ_{02}) asymmetries. The MDS solution for voice quality of the ξ_{02} samples is shown in Figure 9a. The most asymmetric sample (sample 1; ξ_{02} = 0.4 cm) anchors the figure on the left, and the most overcorrected ξ_{02} (sample 15; ξ_{02} = −0.08 cm) anchors the figure on the right. In general, listeners perceived each 0.03-cm ξ_{02} increment as different and each movement toward (or past) midline as successively better. Two measures—H1*-H2* and B0-B2—explained significant variance in the MDS coefficients; adjusted r^2 = .994, $F(1, 12) = 1157.600$, $p < .05$. Both measures correlated highly ($r > .9$) with one another and with MFDR.

Bulging (ξ_b) asymmetries. Voice quality improved as ξ_b increased from −0.05 cm (sample 1) to 0.14 cm (sample 15; see Figure 9b). With a few exceptions, each 0.01-cm increase in ξ_b led to improved voice quality. One measure—B0-B2—explained significant variance in the MDS coefficients; adjusted r^2 = .966, $F(1, 13) = 399.483$, $p < .05$. B0-B2 correlated highly ($r > .9$) with each of the five remaining measures.

Figure 5. Changes in vocal function measures with increasing left bulging (ξ_b): (a) maximum flow declination rate (MFDR), (b) the amplitude difference of the first and second harmonics, corrected for the amplitude of the first formant (H1*-H2*), (c) the amplitude difference of two frequency bands, B0 and B1 (B0-B1), (d) the amplitude difference of two frequency bands, B0 and B2 (B0-B2), (e) cepstral peak prominence (CPP), and (f) harmonics-to-noise ratio (HNR).

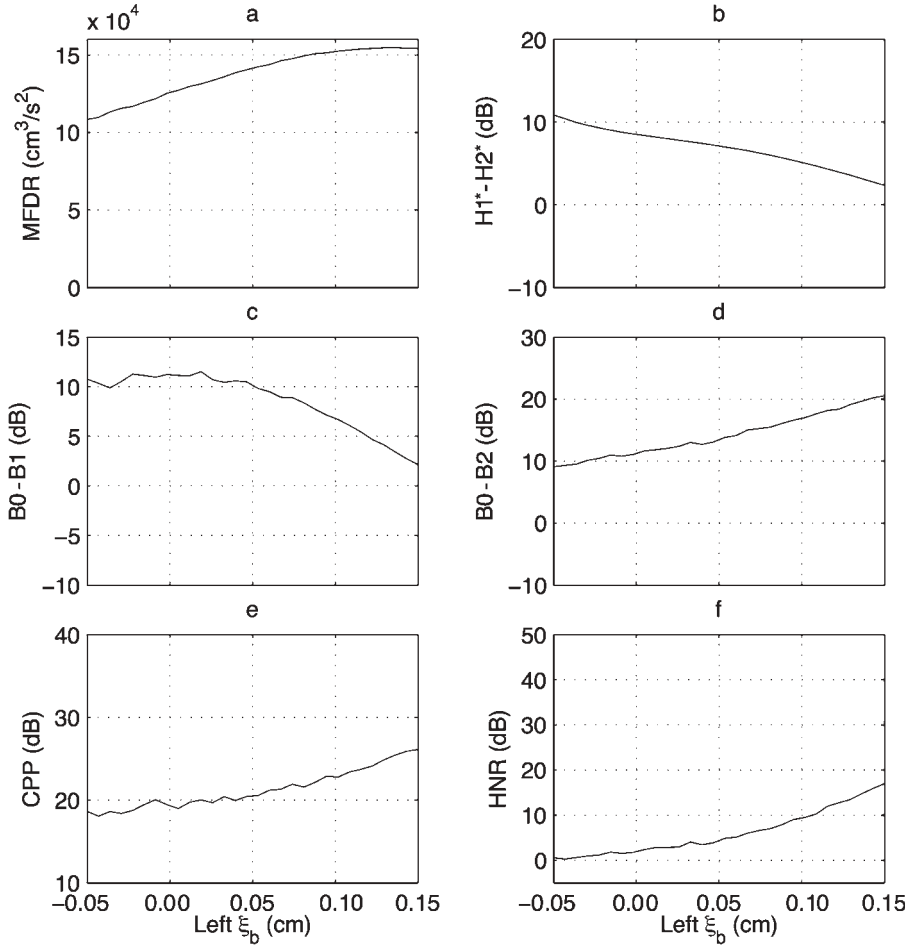

Nodal point ratio (R_{zn}) asymmetries. In general, voice quality was perceived as the worst when R_{zn} was .21 to .38 (samples 3 through 6; see Figure 9c) and best when R_{zn} was .82 to .87 (samples 14 and 15). R_{zn} of .54 to .65 (samples 9 through 11) was perceived to be between the two extremes. B0-B2 best explained the MDS coefficients —adjusted r^2 = .939, $F(1, 13)$ = 215.754, $p < .05$—and correlated highly ($r > .9$) with H1*-H2*, CPP, and HNR.

Amplitude of vibration (Asym) asymmetries. Listeners perceived differences in voice quality as left Asym was altered (see Figure 9d). Although voice quality did not improve in a monotonic manner as left amplitude increased to that of the right, the vowels rated as worst were simulated using the smallest left-sided amplitudes (Asym ≤ .14), and the vowels identified as best were simulated using higher vibratory amplitudes (Asym ≥ .76). The measure MFDR explained the most variance for Asym ratings; adjusted r^2 = .907, $F(1, 13)$ = 137.665, $p < .05$. MFDR correlated highly ($r > .9$) with H1*-H2*, B0-B2, and CPP.

Starting phase (φ) asymmetries. Although raters perceived differences in voice quality with incremental changes to left phase symmetry (see Figure 9e), they did not perceive a monotonic improvement with increased symmetry. The most asymmetric φ (i.e., left φ = 2.4–2.1 radians) produced the worst voice quality. The voice perceived as best was not simulated using symmetric φ but with left φ of 0.41 radians. Vowels simulated with more symmetric φ settings (φ = 0.91–0.08 radians) were rated as better than those that were less symmetric, and the largest changes between adjacent samples occurred for intermediate φ values (φ = 2.07–0.91 radians). Together, H1*-H2* and B0-B2 explained significant variance in the MDS coordinates; adjusted r^2 = .982, $F(1, 13)$ = 389.859, $p < .05$. H1*-H2* and B0-B2 correlated highly ($r > .9$) with one another and with MFDR, CPP, and HNR.

Relative influence of model parameters on perceptual rating. The relative influence of each of the model parameters on perceived overall voice quality was assessed through the

Figure 6. Changes in vocal function measures with increasing left nodal point ratio (R_{zn}): (a) maximum flow declination rate (MFDR), (b) XXXX (H1*-H2*), (c) XXXX (B0-B1), (d) XXXX (B0-B2), (e) cepstral peak prominence (CPP), and (f) harmonics-to-noise ratio (HNR).

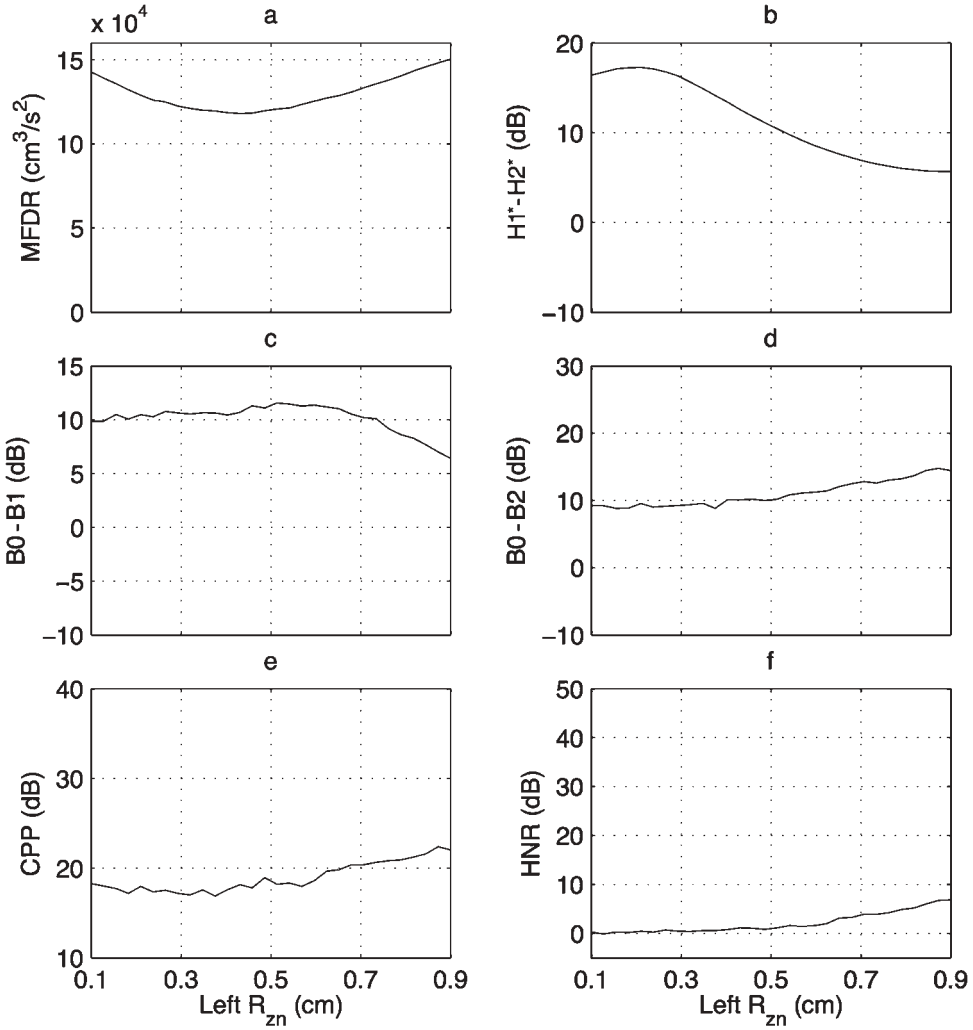

sixth sort-and-rate task. Again, a one-dimensional solution adequately explained the variability in listener results (dispersion accounted for = 0.97). As observed in Figure 10, ξ_{02} (rust-colored markers) had the most substantial influence on voice quality, with the highest rating occurring for the vowel simulated with the left process crossing midline ($\xi_{02} = -0.08$ cm, A3) and the lowest rating occurring for the vowel in which the left process was set farthest from midline ($\xi_{02} = 0.4$ cm, A1). High ξ_b (B3, green marker), high R_{zn} (N3, blue marker), medium ξ_b (B2), and increased phase symmetry (P3, purple marker) were rated as improving voice quality relative to the vowel in which the configuration was closest to baseline (V3, pink marker). Other modifications worsened voice quality relative to V3. Low or medium R_{zn} (N1, N2), decreased ξ_b (B1), and a medium reduction in left Asym (V2) worsened quality to a smaller extent, whereas increasing the distance of the left vocal process from midline (A2), large left–right phase difference (P1), and elimination of left vibratory amplitude (V1) worsened quality to a larger degree. Audio and video samples from the highest and lowest values of each parameter modification can be found in the online supplemental materials (see the following: Supplemental Audio S3, Supplemental Video S3; Supplemental Audio S4, Supplemental Video S4; Supplemental Audio S5, Supplemental Video S5; Supplemental Audio S6, Supplemental Video S6; Supplemental Audio S7, Supplemental Video S7; Supplemental Audio S8, Supplemental Video S8; Supplemental Audio S9, Supplemental Video S9; Supplemental Audio S10, Supplemental Video S10; Supplemental Audio S11, Supplemental Video S11; Supplemental Audio S12, Supplemental Video S12).

Stepwise liner regression showed that ξ_{02}, ξ_b, and vibratory amplitude explained a significant amount of variance in the MDS solution; adjusted $r^2 = .650$, $F(1, 11) = 9.839$, $p < .05$. Three vocal function measures (H1-H2, MFDR, and HNR) together explained significant variance in

Figure 7. Changes in vocal function measures with increasing left amplitude of vibration (Asym): (a) maximum flow declination rate (MFDR), (b) XXXX (H1*-H2*), (c) XXXX (B0-B1), (d) XXXX (B0-B2), (e) cepstral peak prominence (CPP), and (f) harmonics-to-noise ratio (HNR).

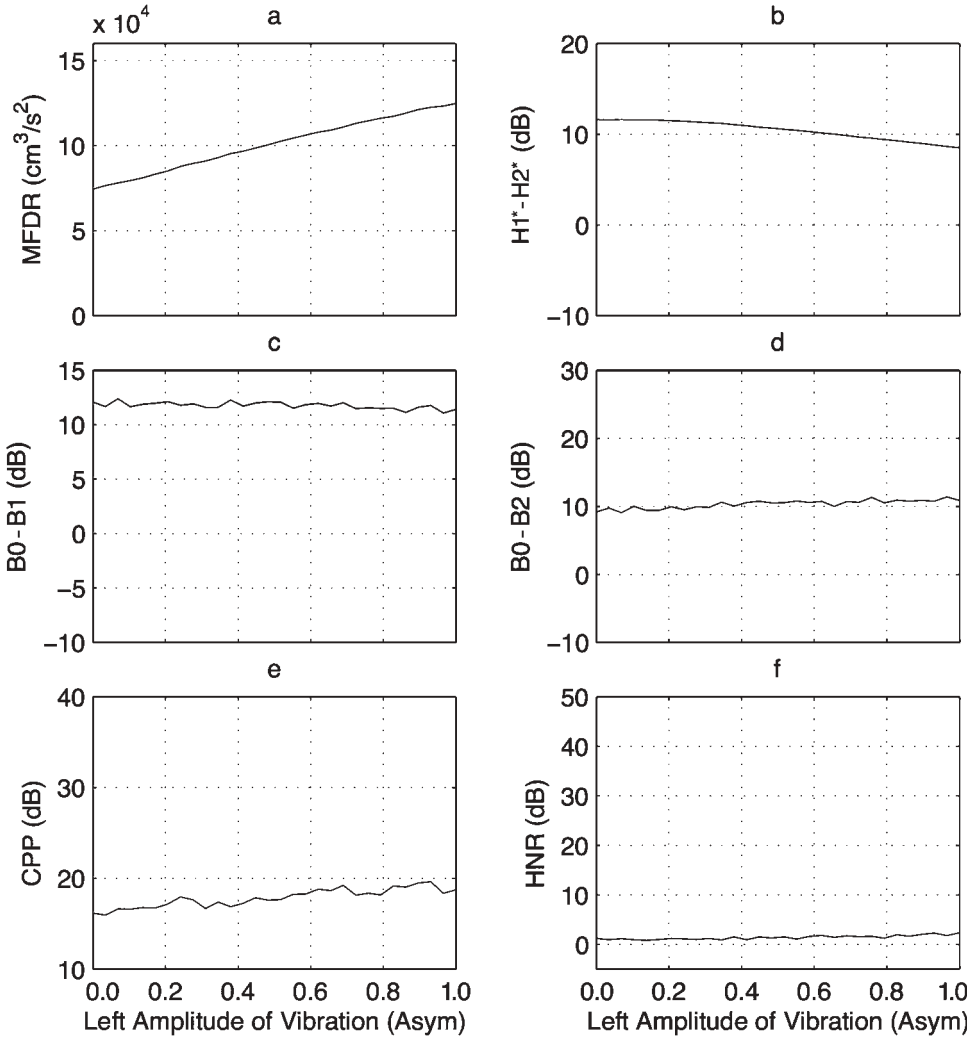

the MDS solution; adjusted $r^2 = .941$, $F(1, 11) = 75.353$, $p < .05$.

Discussion

A computational model was used to vary individual anatomic or kinematic features of the vocal folds, alone and in combination, and determine the effects of each feature on vocal function and voice quality. In Experiment 1, we determined that small left–right asymmetries of bulging, nodal point ratio, and starting phase negatively changed vocal function, even in the context of symmetric vocal process adduction. The changes that occurred in the A_g, U_g, and P_{out} signals were similar to those described for breathy voice by Fischer-Jørgensen (1967), Hillenbrand et al. (1994), Huffman (1987), and Klatt and Klatt (1990) and summarized in the introduction. The vocal fold surfaces closed the glottal airspace slightly less than in the symmetric exemplar even though the vocal process adduction values were identical for the two exemplars. To determine whether the incomplete closure was primarily the result of decreased ξ_b, R_{zn}, or φ, the minimum area of the asymmetric exemplar was compared in cases where only one of the three asymmetries was present. The minimum area for the exemplar (0.0209 cm^2) was higher than for any of the individual components (0.0113 cm^2 for ξ_b, 0.0040 for R_{zn}, and 0.0024 for φ), demonstrating that the A_g changes were not the result of just a single component parameter.

The A_g and U_g skewing quotients were lower for the asymmetric exemplar, reflecting slower decreases in area and flow than occurred for the symmetric exemplar. The U_g skewing that occurs secondary to interaction with pressures of the sub- and supraglottal vocal tract was weaker for the asymmetric exemplar, the consequences of which were illustrated in the asymmetric exemplar's steeper spectral slope. Taken together, these changes indicate that the

Figure 8. Changes in vocal function measures with decreasing left starting phase (φ): (a) maximum flow declination rate (MFDR), (b) The amplitude difference of the first and second harmonics, corrected for the amplitude of the first formant (H1*-H2*), (c) The amplitude difference of two frequency bands, B0 and B1 (B0-B1), (d) The amplitude difference of two frequency bands, B0 and B2 (B0-B2), (e) cepstral peak prominence (CPP), and (f) harmonics-to-noise ratio (HNR).

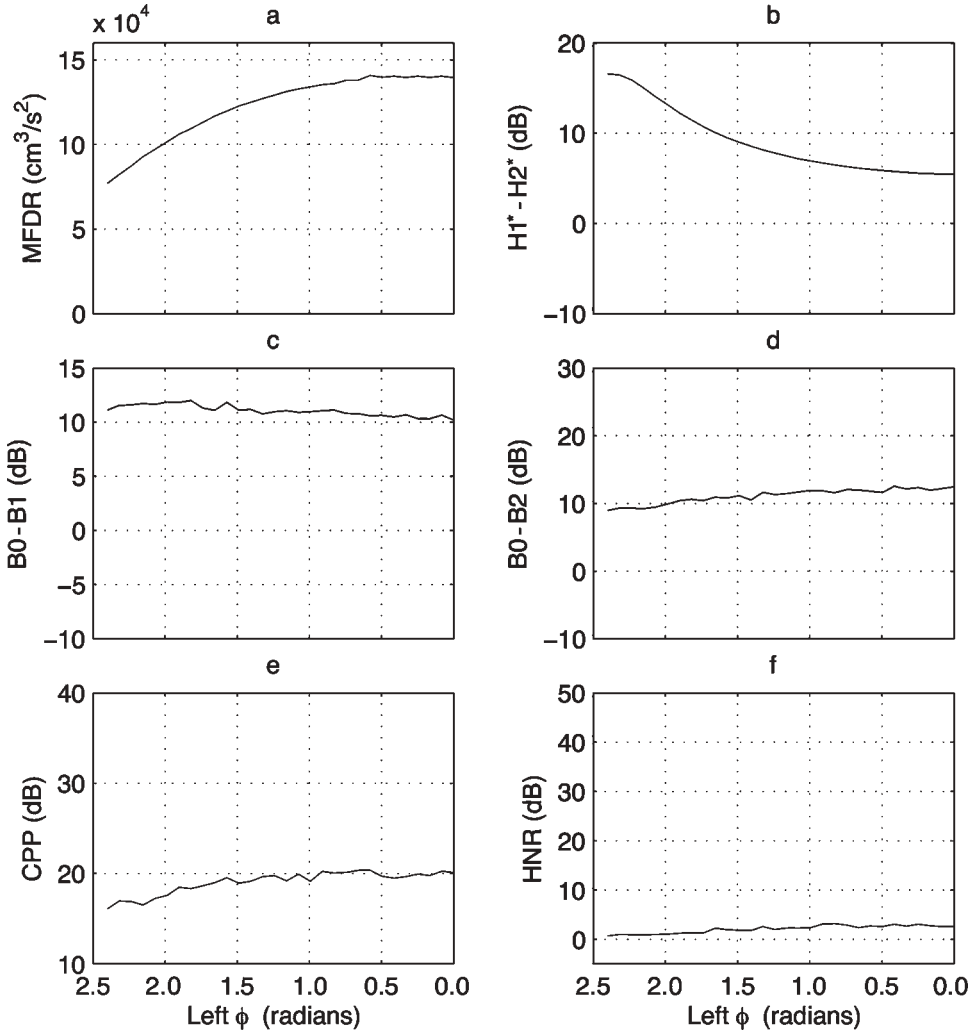

Table 4. Comparison of best (maximum or minimum) vocal function measures across parameters.

Parameter	Maximum MFDR (cm^3/s^2)	Minimum H1*-H2* (dB)	Minimum B0-B1 (dB)	Maximum B0-B2 (dB)	Maximum CPP (dB)	Maximum HNR (dB)
ξ_{02}	**156,180**	**–2.9**	**–4.8**	**26.6**	**35.9**	**42.8**
ξ_b	154,606	2.4	2.1	20.5	26.1	17.0
R_{zn}	150,316	5.7	6.4	14.4	22.4	6.8
Asym	*124,777*	*8.5*	*11.1*	*11.4*	*19.6*	*2.3*
φ	140,353	5.4	10.1	12.5	20.1	3.1

Note. The best value for each measure is in bold font, and the worst value is in italic font. MFDR = maximum flow declination rate; H1*-H2* = XXX; B0-B1 = XXX; B0-B2 = XXX; CPP = cepstral peak prominence; HNR = harmonics-to-noise ratio; ξ_{02} = adduction; ξ_b = bulging; R_{zn} = nodal point ratio; Asym = asymmetry; φ = starting phase.

Figure 9. Perceived voice quality with changes in model parameters: (a) adduction, (b) bulging, (c) nodal point ratio, (d) asymmetry, and (e) starting phase.

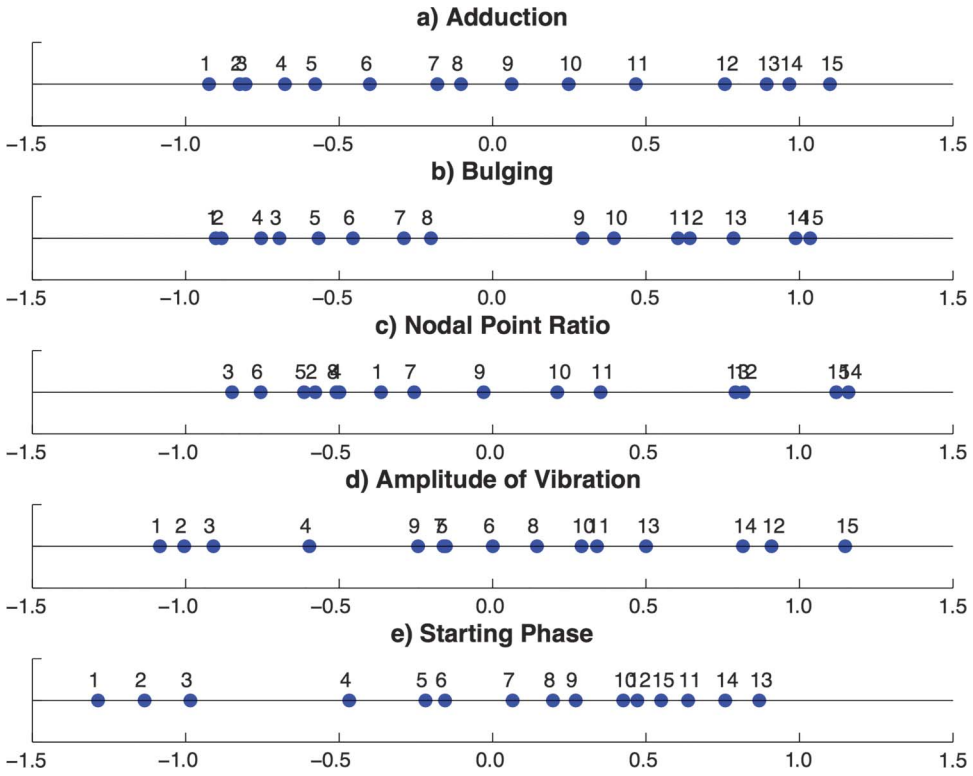

combination of three small asymmetries (ξ_b, R_{zn}, and φ) modified the voice signal in a manner consistent with breathy voice quality.

The asymmetric exemplar used in Experiment 1 became the basis for Experiment 2, in which individual model parameters were manipulated to determine how they worsened and improved the vocal function and voice quality of the asymmetric exemplar. Although all five parameters influenced vocal function and voice quality, the largest and most consistent improvements occurred with "overcorrection" of adduction (i.e., moving ξ_{02} from the symmetric value of 0.1 cm to, and slightly past, midline). Overcorrection of bulging resulted in the next highest improvement, followed by increased symmetry of nodal point ratio, starting phase, and amplitude of vibration. Highly asymmetric adduction, decreased phase symmetry, and decreased left amplitude of vibration worsened voice quality. Despite the finding that a 0.1-cm overcorrection improved voice more than midline placement, cautious clinical interpretation is recommended given that overcorrection might lead to patient sensations (e.g., fullness, need to clear throat) that would limit benefit.

Even though some changes in quality were likely larger than others, naïve listeners were able to distinguish differences in voice quality with manipulation of each parameter. The changes to voice quality with adduction, bulging, and amplitude of vibration were almost monotonic in that almost every increment of parameter setting in the direction hypothesized to improve voice resulted in better voice quality. This was not the case for changes to nodal point ration or phase, although

Figure 10. Perceived voice quality changes across model parameters: multidimensional scaling solution where A = adduction, B = bulging, N = nodal point ratio, V = asymmetry (amplitude of vibration), and P = phase. A letter followed by the number 1 is the most asymmetric of that parameter, a letter followed by the number 2 is the midpoint value of that parameter, and a letter followed by the number 3 is the most symmetric or overcorrected value of that parameter.

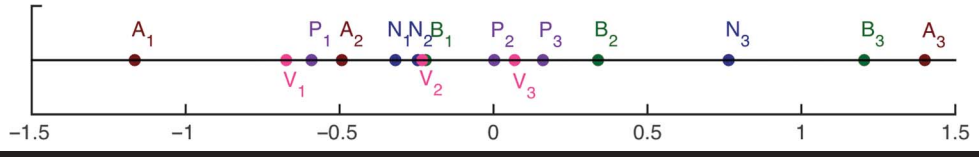

there were patterns of better voice with higher nodal point ratio and more phase symmetry and worse voice with lower bulging and less phase symmetry. The finding that each parameter negatively and positively influenced voice quality and vocal function augments the understanding of asymmetry gained from Samlan et al. (2014), demonstrating the importance of the context of a particular asymmetry. Unilateral amplitude and phase asymmetries have more influence on voice quality when other asymmetries are present than when amplitude of phase is the sole asymmetry.

The current study demonstrated one context in which amplitude and φ asymmetries are perceptually important. Even though setting the adduction and bulging values to cross midline overrode the effects of the other three asymmetries, nodal point ratio, amplitude, and phase asymmetries affected voice quality when glottal closure was less complete. The findings are consistent with the current surgical approach to VFMI in which goals include medializing the vocal process and straightening concave edges. The results also explain many of the residual voice limitations postoperatively. The findings provide direction to clinicians in that working toward improving the remaining asymmetries should further improve voice quality in patients with VFMI.

As discussed in the introduction, differences in left–right φ and Asym might be expected as part of normal left–right asymmetries in human bodies and behavior, although asymmetry is also a hallmark of disordered vocal fold patterns. As part of a constellation of mild asymmetries in the current study, however, phase and amplitude asymmetries increased dysphonia and worsened measures of vocal function beyond what was achieved with any of the asymmetries alone. Improving phase and amplitude asymmetries improved voice quality, even in the context of other asymmetries. The discussion below highlights how the five asymmetries investigated (ξ_{02}, ξ_b, R_{zn}, phase, and amplitude) are likely mitigated using current treatments for VFMI.

Medical treatments that might improve laryngeal nerve regeneration in some cases of unilateral VFMI are under investigation (Hydman, Björck, Persson, Zedenius, & Mattsson, 2009; Hydman, Remahl, Björck, Svensson, & Mattsson, 2007; Mattsson et al., 2005; Mori et al., 2007; Rosen et al., 2014; Sridharan, Rosen, Smith, Young, & Munin, 2015), although surgical treatment to improve voice quality remains the standard of care. Surgical approaches fall into the general categories of arytenoid adduction, medialization (e.g., injection or thyroplasty), and reinnervation. Each type of treatment might alter multiple vocal fold structure and kinematic properties through different mechanisms. Arytenoid adduction would primarily alter vocal process adduction, possibly resulting in a straight (as opposed to concave) bulging value, increased amplitude of vibration, and decreased left–right phase difference (φ; Kokesh et al., 1993). The goal for medialization thyroplasty and injection laryngoplasty is typically improved ability of the vocal folds to close the glottal airspace through medial displacement of the membranous vocal fold, changing the contour of the medial edge (ξ_{02} and ξ_b parameters of the kinematic model). As with arytenoid adduction, improved ability to close the airspace might also improve amplitude of vibration and phase. In addition, it is likely that the distribution of mass, shape of the edge thickness (e.g., convergent, divergent, or rectangular), muscle activation, and aerodynamic quantities influence the nodal point ratio. Nerve regeneration, either through surgically guided reinnervation or spontaneous postinjury regeneration, is the only method for restoring neurologic input to the immobilized thyroarytenoid muscle. The resulting central input, corresponding with the intact neurologic signals to the contralateral vocal fold, may offer the greatest likelihood of correcting residual nodal point, phase, and amplitude asymmetries, which appear to be important in perception of poor voice quality in a minimally asymmetric model with adequate glottal closure.

Further investigation is necessary to better predict the effects of individual or combinations of asymmetries on voice when other asymmetries are more substantial. Future directions would also include investigation of how the vertical location of increased bulging affects vocal function.

Acknowledgments

We thank the Bureau of Glottal Affairs, UCLA Department of Head and Neck Surgery, for the Sort and Rate Software.

References

Alipour, F., & Scherer, R. C. (2000). Vocal fold bulging effects on phonation using a biophysical computer model. *Journal of Voice, 14*(4), 470–483.

American Speech-Language-Hearing Association. (1997). *Guidelines for audiologic screening*. Retrieved from http://www.asha.org/policy

Bielamowicz, S., Kapoor, R., Schwartz, J., & Stager, S. V. (2004). Relationship among glottal area, static supraglottic compression, and laryngeal function studies in unilateral vocal fold paresis and paralysis. *Journal of Voice, 18,* 138–145.

Billante, C. R., Clary, J., Childs, P., & Netterville, J. L. (2002). Voice gains following thyroplasty may improve over time. *Clinical Otolaryngology, 27,* 89–94.

Boersma, P. (1993). Accurate short-term analysis of the fundamental frequency and the harmonics-to-noise ratio of a sampled sound. *Institute of Phonetic Sciences Proceedings, 17,* 97–110.

Boersma, P., & Weenink, D. (2011). Praat: Doing Phonetics by Computer (Version 5.2.40) [Computer program]. Retrieved from http://www.praat.org/

de Krom, G. (1995). Some spectral correlates of pathological breathy and rough voice quality for different types of vowel fragments. *Journal of Speech and Hearing Research, 38,* 794–811.

Esposito, C. M. (2010). The effects of linguistic experience on the perception of phonation. *Journal of Phonetics, 38,* 306–316.

Eysholdt, U., Rosanowski, F., & Hoppe, U. (2003). Vocal fold vibration irregularities caused by different types of laryngeal asymmetry. *European Archives of Otorhinolaryngology, 260,* 412–417.

Fischer-Jørgensen, E. (1967). Phonetic analysis of breathy (murmured) vowels in Gujarti. *Indian Linguistics, 28,* 71–139.

Granqvist, S. (2003). The visual sort and rate method for perceptual evaluation in listening tests. *Logopedics Phoniatrics Vocology, 28,* 109–116.

Gray, S. D., Barkmeier, J., Jones, D., Titze, I., & Druker, D. (1992). Vocal evaluation of thyroplastic surgery in the treatment of unilateral vocal fold paralysis. *Laryngoscope, 102,* 415–421.

Hanson, H. (1997). Glottal characteristics of female speakers: Acoustic correlates. *The Journal of the Acoustical Society of America, 101,* 466–481.

Hartl, D., Hans, S., Vaissière, J., & Brasnu, D. (2003). Objective acoustic and aerodynamic measures of breathiness in paralytic dysphonia. *European Archives of Oto-Rhino-Laryngology, 260,* 175–182.

Hillenbrand, J., Cleveland, R., & Erickson, R. (1994). Acoustic correlates of breathy vocal quality. *Journal of Speech and Hearing Research, 37,* 769–778.

Hirano, M., & Mori, K. (2000). Vocal fold paralysis. In R. D. Kent & M. J. Ball (Eds.), *Voice quality measurement* (pp. 385–396). San Diego, CA: Singular.

Hogikyan, N. D., Wodchis, W. P., Terrell, J. E., Bradford, C. R., & Esclamado, R. M. (2000). Voice-related quality of life (V-RQOL) following type I thyroplasty for unilateral vocal fold paralysis. *Journal of Voice, 143,* 378–386.

Huffman, M. (1987). Measures of phonation type in Hmong. *The Journal of the Acoustical Society of America, 81,* 495–504.

Hydman, J., Björck, G., Persson, J. K., Zedenius, J., & Mattsson, P. (2009). Diagnosis and prognosis of iatrogenic injury of the recurrent laryngeal nerve. *Annals of Otology, Rhinology & Laryngology, 118,* 506–511.

Hydman, J., Remahl, S., Björck, G., Svensson, M., & Mattsson, P. (2007). Nimodipine improves reinnervation and neuromuscular function after injury to the recurrent laryngeal nerve in the rat. *Annals of Otology, Rhinology & Laryngology, 116,* 623–630.

Isshiki, N., & Ishikawa, T. (1976). Diagnostic value of tomography in unilateral vocal cord paralysis. *Laryngoscope, 86,* 1573–1578.

Klatt, D., & Klatt, L. (1990). Analysis, synthesis, and perception of voice quality variations among female and male talkers. *The Journal of the Acoustical Society of America, 87,* 820–857.

Kiritani, S., Hirose, H., & Imagawa, H. (1993). High-speed digital image analysis of vocal cord vibration in diplophonia. *Speech Communication, 13,* 23–32.

Kokesh, J., Flint, P. W., Robinson, L. R., & Cummings, C. W. (1993). Correlation between stroboscopy and electromyography in laryngeal paralysis. *Annals of Otology, Rhinology & Laryngology, 102,* 852–857.

Leder, S. B., & Sasaki, C. T. (1994). Long-term changes in vocal quality following Isshiki thyroplasty type I. *Laryngoscope, 104*(3 Pt. 1), 275–277.

Liljencrants, J. (1985). *Speech synthesis with a reflection-type line analog* (Unpublished doctoral dissertation). Royal Institute of Technology, Stockholm, Sweden.

Lohscheller, J., & Eysholdt, U. (2008). Phonovibrogram visualization of entire vocal fold dynamics. *Laryngoscope, 118,* 753–758.

Lundy, D. S., Casiano, R. R., McClinton, M. E., & Xue, J. W. (2003). Early results of transcutaneous injection laryngoplasty with micronized acellular dermis versus type-I thyroplasty for glottic incompetence dysphonia due to unilateral vocal fold paralysis. *Journal of Voice, 17,* 589–595.

Mattsson, P., Björck, G., Remahl, S., Bäckdahl, M., Hamberger, B., Hydman, J., & Svensson, M. (2005). Nimodipine and microsurgery induced recovery of the vocal cord after recurrent laryngeal nerve resection. *Laryngoscope, 115,* 1863–1865.

Mori, Y., Shiotani, A., Saito, K., Araki, K., Ikeda, K., Nakagawa, M., . . . Ogawa, K. (2007). A novel drug therapy for recurrent laryngeal nerve injury using T-588. *Laryngoscope, 117,* 1313–1318.

Omori, K., Slavit, D., Kacker, A., Blaugrund, S., & Kojima, H. (2000). Effects of thyroplasty type I on vocal fold vibration. *Laryngoscope, 110,* 1086–1091.

Pinho, S. M., Pontes, P. A., Gadelha, M. E., & Biasi, N. (1999). Vestibular vocal fold behavior during phonation in unilateral vocal fold paralysis. *Journal of Voice, 13,* 36–42.

Rosen, C. A., Smith, L., Young, V., Krishna, P., Muldoon, M. F., & Munin, M. C. (2014). Prospective investigation of nimodipine for acute vocal fold paralysis. *Muscle & Nerve, 50,* 114–118. doi:10.1002/mus.24111

Samlan, R. A., & Kreiman, J. (2014). Perceptual consequences of changes in epilaryngeal area and shape. *The Journal of the Acoustical Society of America, 136*(5), 2798–2806.

Samlan, R. A., & Story, B. H. (2011). Relation of structural and vibratory kinematics of the vocal folds to two acoustic measures of breathy voice based on computational modeling. *Journal of Speech, Language, and Hearing Research, 54,* 1267–1283.

Samlan, R. A., Story, B. H., & Bunton, K. (2013). Relation of perceived breathiness to laryngeal kinematics and acoustic measures based on computational modeling. *Journal of Speech, Language, and Hearing Research, 56,* 1209–1223.

Samlan, R. A., Story, B. H., Lotto, A. J., & Bunton, K. (2014). The acoustic and perceptual effects of left-right vocal fold asymmetries based on computational modeling. *Journal of Speech, Language, and Hearing Research, 57,* 1619–1637.

Schwarz, R., Hoppe, U., Schuster, M., Wurzbacher, T., Eysholdt, U., & Lohscheller, J. (2006). Classification of unilateral vocal fold paralysis by endoscopic digital high-speed recordings and inversion of a biomechanical model. *IEEE Transactions on Biomedical Engineering, 53,* 1099–1108.

Shue, Y., Keating, P., Vicenik, C., & Yu, K. (2011). VoiceSauce: A program for voice analysis. *ICPhS Proceedings, 17,* 1846–1849.

Sridharan, S. S., Rosen, C. A., Smith, L. J., Young, V. N., & Munin, M. C. (2015). Timing of nimodipine therapy for the treatment of vocal fold paralysis. *The Laryngoscope, 125,* 186–190. doi:10.1002/lary.24903

Story, B. H. (1995). *Speech simulation with an enhanced wave-reflection model of the vocal tract* (Unpublished doctoral dissertation). University of Iowa, Iowa City.

Story, B. H. (2005). A parametric model of the vocal tract area function for vowel and consonant simulation. *The Journal of the Acoustical Society of America, 117,* 3231–3254.

Story, B. H. (2008). Comparison of magnetic resonance imaging-based vocal tract area functions obtained from the same speaker in 1994 and 2002. *The Journal of the Acoustical Society of America, 123,* 327–335.

Thompson, D. M., Maragos, N. E., & Edwards, B. E. (1995). The study of vocal fold vibratory patterns in patients with unilateral vocal fold paralysis before and after type I thyroplasty with or without arytenoid adduction. *Laryngoscope, 105,* 481–486.

Titze, I. R. (1984). Parameterization of the glottal area, glottal flow, and vocal fold contact area. *The Journal of the Acoustical Society of America, 75,* 570–580.

Titze, I. R. (1989). A four-parameter model of the glottis and vocal fold contact area. *Speech Communication, 8,* 191–201.

Titze, I. R. (2002). Regulating glottal airflow in phonation: Application of the maximum power transfer theorem to a low dimensional phonation model. *The Journal of the Acoustical Society of America, 111*(1 Pt. 1), 367–376.

Titze, I. R. (2006). *The myoelastic aerodynamic theory of phonation*. Denver, CO: National Center for Voice and Speech.

Titze, I. R., Horii, Y., & Scherer, R. C. (1987). Some technical considerations in voice perturbation measurements. *Journal of Speech and Hearing Research, 30,* 252–260.

Titze, I. R., & Story, B. H. (2002). Rules for controlling low-dimensional vocal fold models with muscle activation. *The Journal of the Acoustical Society of America, 112*(3), 1064–1076.

von Leden, H., & Moore, P. (1961). Vibratory pattern of the vocal cords in unilateral laryngeal paralysis. *Acta Oto-Laryngologica, 53,* 493–506.

Wittenberg, T., Tigges, M., Mergell, P., & Eysholdt, U. (2000). Functional imaging of vocal fold vibration: Digital multislice high-speed kymography. *Journal of Voice, 14,* 422–442.

Yamada, M., Hirano, M., & Ohkubo, H. (1983). Recurrent laryngeal nerve paralysis. A 10-year review of 564 patients. *Auris Nasus Larynx, 10*(Suppl.), S1–S15.

Yumoto, E., Nakano, K., & Oyamada, Y. (2003). Relationship between 3D behavior of the unilaterally paralyzed larynx and aerodynamic vocal function. *Acta Oto-Laryngologica, 123,* 274–278.